NACA

RESEARCH MEMORANDUM

FLIGHT INVESTIGATION OF THE ZERO-LIFT DRAG OF TWO RAM-JET MISSILE CONFIGURATIONS AT MACH NUMBERS FROM 1.00 TO 1.89

By Clarence A. Brown, Jr., and Walter E. Bressette

Langley Aeronautical Laboratory
Langley Field, Va.

NATIONAL ADVISORY COMMITTEE
FOR AERONAUTICS

WASHINGTON

March 9, 1953

NATIONAL ADVISORY COMMITTEE FOR AERONAUTICS

RESEARCH MEMORANDUM

FLIGHT INVESTIGATION OF THE ZERO-LIFT DRAG OF TWO RAM-JET MISSILE CONFIGURATIONS AT MACH NUMBERS FROM 1.00 TO 1.89

By Clarence A. Brown, Jr., and Walter E. Bressette

SUMMARY

Flight tests using rocket-powered models were conducted to determine the zero-lift drag of two ram-jet missile configurations. The configurations that were tested were an underslung single-inlet ram-jet missile configuration and a two-dimensional twin-inlet ram-jet missile configuration. The external-drag coefficient, based on the cylindrical fuselage cross-sectional area, for the underslung single-inlet ram-jet configuration had a gradual decrease from a value of 0.45 at a Mach number of 1.00 to 0.38 at a Mach number of 1.60. The corresponding Reynolds numbers based on body length were 45×10^6 and 84×10^6. The external-drag coefficient for the two-dimensional twin-inlet ram jet had a gradual increase from a value of 0.48 at a Mach number of 1.10 to a peak of 0.56 at a Mach number of 1.37 and then varied smoothly to a value of 0.47 at a Mach number of 1.89. The corresponding Reynolds numbers were 56×10^6 and 130×10^6.

Qualitative comparison of the flight-test data with data from a twin-nacelle ram jet indicates no appreciable difference in the external-drag coefficient between the different installations of the ram-jet engines on the models of similar geometric size and volume.

INTRODUCTION

Recently there has been considerable interest in ram-jet engines and the drag of ram-jet configurations has become increasingly important. To determine the thrust requirements of a configuration, the drag characteristics must be evaluated.

This paper presents the zero-lift external drag of an underslung single-inlet ram-jet missile configuration and a two-dimensional

twin-inlet ram-jet missile configuration as obtained from the rocket-powered technique. The designs of these two ram-jet configurations were independent of each other although the inlet areas, combustion areas, and exit areas of the two configurations were equal. The inlets of the two models differed in that the underslung single-inlet configuration had a single diffuser located beneath and near the fuselage of the model whereas the two-dimensional twin-inlet configuration had two diffusers located in the leading edges of the horizontal wings. For the two-dimensional ram jet, preliminary tests indicated that the pressure recovery would be sufficient for operation with this type of inlet.

The Mach number range covered by the underslung single-inlet ram-jet configuration was 1.00 to 1.60 and the Reynolds number, based on the total body length, varied from 45×10^6 to 84×10^6. The Mach number range covered by the two-dimensional twin-inlet ram-jet configuration was 1.10 to 1.89 and the Reynolds number, based on total body length, varied from 56×10^6 to 130×10^6.

SYMBOLS

C_D	drag coefficient, $\frac{\text{Drag}}{qS_b}$
C_{N_w}	normal-force coefficient, $\frac{\text{Normal force}}{qS_w}$
S_b	cross-sectional area of cylindrical section of fuselage, sq ft
S_w	exposed wing area of model A, sq ft
p_2	duct exit pressure, lb/sq in. abs
p_b	base pressure, lb/sq in. abs
p_o	free-stream static pressure, lb/sq in. abs
V	velocity of model, ft/sec

γ	ratio of specific heats (1.40)
M	Mach number
q	dynamic pressure, lb/sq ft
R	Reynolds number, $\frac{Vl}{\nu}$
l	length of model, ft
ν	kinematic viscosity, sq ft/sec
A_o	free-stream tube area
A_1	geometric entrance area (maximum capture area) of ram-jet inlet (model A, 0.0491 sq ft; model B, 0.0481 sq ft)
A_2	exit area of ram jet (model A, 0.0562 sq ft; model B, 0.0562 sq ft)

APPARATUS AND METHODS

Model Description

Sketches of the rocket-powered models used in these tests are shown in figures 1 and 2. Photographs of the models are shown as figures 3 and 4. The models were of composite wood-metal construction and a coating of Phenoplast (ref. 1) was applied to the wood to withstand the temperature reached in flight due to aerodynamic heating.

Each model was boosted to supersonic velocities by a solid-propellant rocket motor which delivered approximately 6,000 pounds of thrust for 3.0 seconds. The underslung single-inlet configuration was launched at an angle of approximately 45° to the horizontal whereas the two-dimensional twin-inlet configuration was launched at an angle of approximately 60° to the horizontal.

In the design of the two models, the total frontal area was kept to a minimum by submerging the ram-jet engine in the after part of each of the bodies. For the single-inlet ram jet, the total frontal area of the inlet plus fuselage was approximately 70 percent greater than the frontal area of the fuselage alone and, for the two-dimensional twin-inlet ram jet, the total frontal area of the fuselage, inlet, and wing was approximately 47 percent greater than the frontal area of the fuselage plus wing. The two models had single exits and the exit areas were equal.

The inlets of the models differed inasmuch as, in the case of the underslung single-inlet ram jet, the air entered the diffuser and was ducted into the body of the model and out the single exit at the rear of the model. In the case of the two-dimensional twin-inlet ram jet, however, the air entered the two diffusers located in the leading edges of the wing and was ducted into the body of the model and out the single exit at the rear of the model.

Underslung single-inlet ram jet.- The body of model A had a maximum diameter of 5 inches with a fineness ratio of 18.04. The fuselage was cylindrical with a 5° semiangle conical nose and a blunt base. Canard surfaces were located on the nose cone of the model and the vertical canard surfaces were positioned ahead of the horizontal canard surfaces (fig. 1). The canard surfaces were of 70° delta wing plan form and a hexagonal airfoil section having a constant thickness ratio of 4 percent. The maximum thickness extended from 45.6 percent chord to 78.2 percent chord. The horizontal canard surfaces were deflected 2° to trim the model near zero lift. The horizontal wings were of 65° delta plan form with a modified hexagonal airfoil section of constant thickness corresponding to a thickness ratio of 2.3 percent at the wing-body juncture. The maximum thickness at the wing-body juncture extended from 19.2 percent chord to 83.9 percent chord. The horizontal wing differed from a true delta wing by sweeping forward the trailing edge of the wing tip. The vertical wings were of 65° delta plan form with a hexagonal airfoil section with a constant thickness ratio of 3.68 percent. The maximum thickness extended from 39 percent chord to 61 percent chord. The single ram jet was underslung and both the fuselage and diffuser were canted to reduce the length of the forward section of the ram jet. A sectional view of the fuselage-duct intersection is shown in figure 5. A fillet was positioned ahead of the fuselage-duct intersection in an attempt to reduce the drag (fig. 5). The internal geometry of the diffuser and location of the orifices for measuring the duct and base pressure are also shown in figure 5. The duct static pressure was taken in six places around the inside of the duct and manifolded together whereas the base pressure was taken in six places around the base of the duct and manifolded together. A restriction was placed near the end of the duct so that sonic velocity would be present at the exit of the duct at supersonic speed.

Two-dimensional twin-inlet ram-jet.- The body of model B had a maximum diameter of 5 inches with a fineness ratio of 24.70. The fuselage was cylindrical with a 4.1° semiangle conical nose and a blunt base (fig. 2). The vertical wing of model B was of rectangular plan form with a modified hexagonal section and the leading and trailing edges swept back 45°. The maximum thickness ratio of 1.85 percent at the wing-body juncture extended from 10.4 percent chord to 88.9 percent chord. The vertical wing of model B had a thickness ratio that varied from 1.85 percent at the wing-body juncture to 0 percent at the wing tip. The

horizontal wing was of rectangular plan form with the two-dimensional inlets located in the leading edges (fig. 6). In order to accommodate the two-dimensional inlets in the leading edges of the horizontal wing, the thickness of the wing was increased to five times the thickness of the vertical wing at the wing-body juncture. A ramp-type fillet was positioned between the body and the inlet to keep the boundary layer of the body from entering the inlet (fig. 6). Figure 6 shows the internal geometry of the two-dimensional twin-inlets and locations of the manifolded total-pressure rake used in measuring the total pressure at the sonic exit. Turning vanes in the ducts, which would be required to maintain good recovery, were considered irrelevant to this drag model and were, therefore, not included. Also shown in figure 6 is the location of the base-pressure orifice. The two inlets contained protruding wedges that had a total angle of 24°. This wedge angle was selected so that at a design speed of $M = 1.80$ the pressure recovery would be near optimum. The wedges protruded forward a distance which would cause the oblique shock wave to intercept the entrance at the design Mach number.

Instrumentation

Model A was equipped with a four-channel telemeter which transmitted a continuous record of normal and longitudinal accelerations and base and duct pressures. The base pressure was taken on the base of the duct whereas the duct exit pressure was taken inside and near the rear end of the duct (fig. 5).

Model B was equipped with a four-channel telemeter which transmitted a continuous record of longitudinal (two ranges) acceleration, a manifolded total pressure in the duct, and base pressure. Internal pressure was measured by the manifolded total-pressure rake located near the end of the duct whereas base-pressure measurements were made at the rear of the duct as shown in figure 6.

Velocity was obtained from CW Doppler radar and by integration of the data from the longitudinal accelerometers. Trajectory and atmospheric data were obtained from a tracking radar unit and by radiosonde observation.

Method of Analysis

In order to find the external drag of the configuration, the total drag of the model was measured and the contribution of the internal drag of the ducts and base drag of the model were subtracted. Total drag was obtained during the coasting flight of the models by reduction of the accelerometer record.

Reference 2 gives an analysis of the method used in determining the internal drag. The internal drag of the ducts for models A and B was obtained using the one-dimensional-flow theory applied to the momentum-theorem equation as follows:

$$\text{Internal drag} = p_o A_2 + p_o A_o \gamma M_o^2 - p_2 A_2 \left(1 + \gamma M_2^2\right)$$

where p_o was obtained from radiosonde data for models A and B; p_2 was obtained from manifolded static-pressure pickup near the duct exit for model A and, for model B, p_2 was calculated from the manifolded total-pressure readings taken near the exit of the duct assuming $M_2 = 1$ (ref. 3); M_o was obtained from the CW Doppler radar and radiosonde data for both models A and B; M_2 is assumed to be sonic when the base pressure is less than the internal exit pressure for both models A and B. For both models A and B the ratio of the free-stream tube area to the geometric entrance area was calculated from one-dimensional-flow theory (ref. 2).

The restriction at the exit of the duct resulted in a base area that would not be present in an actual ram jet; therefore, the drag of the base had to be subtracted from the total model drag. The base drag of the models tested was calculated from the base-pressure measurements.

Accuracy

The accuracy of the results, considering possible cumulative errors in radar and telemeter data, is believed to be within the limits listed below:

M, percent	2
C_D	±0.03
C_{N_W}	±0.006

RESULTS AND DISCUSSION

The range of the tests is shown in figure 7 as a plot of Reynolds number variation with Mach number for both models. A plot of the ratio of the model base pressure to the pressure in the duct exit with Mach number is presented in figure 8. As may be seen in figure 8, the pressure ratio for model A was less than 1 throughout the test range, whereas for model B the pressure ratio was less than 1 above a Mach number of 1.10,

which shows both models to have a sonic exit through the Mach number range investigated.

The trim characteristics of model A are shown in figure 9 as the variation of the normal-force coefficient, obtained from the normal accelerometer located at the model center of gravity, with Mach number. Model A was an asymmetric configuration and the positive 2° fixed incidence of the horizontal canard surface was adequate to trim the model near zero lift.

The zero-lift drag characteristics for the single-inlet ram-jet missile configuration (model A) are presented in figure 10 as the variation of the coefficient of the total model drag, internal duct drag, base drag, and external model drag with Mach number. As may be noted in figure 10, the external-model-drag coefficient varied smoothly from a peak value of 0.45 at a Mach number of 1.00 to 0.38 at a Mach number of 1.60 and was approximately 55 to 60 percent of the total model drag throughout the Mach number range investigated.

For model A the calculated free-stream tube area is equal to the entrance area of the inlet and therefore the mass-flow ratio of the inlet is equal to 1.

The zero-lift drag characteristics for the two-dimensional twin-inlet ram-jet missile configuration (model B) is presented in figure 11 as the variation of the coefficient of the total model drag, internal duct drag, base drag, and external model drag with Mach number. The external-model-drag coefficient had a gradual rise from a value of 0.48 at a Mach number of 1.10 to a peak of 0.56 at a Mach number of 1.37 and then varied smoothly to a value of 0.47 at a Mach number of 1.89. The external model drag of model B varied from 55 to 67 percent of the total model drag throughout the Mach number range investigated.

Presented in figure 12 is the variation of the ratio of the free-stream tube area to the geometric entrance area with Mach number. As will be noted in figure 12, the free-stream tube area varied from 95 percent at a Mach number of 1.89 to 76 percent at a Mach number of 1.10. This change in free-stream tube area was caused by the deflection of the air flow behind oblique shock waves from the leading edge of the wedges. At a Mach number of 1.80, the design Mach number of the inlet, the free-stream tube area was not equal to the geometric entrance area as would have been expected. The wedges were constructed so that the ends did not protrude outside the inlet entrance and expansion waves from the tips entered the inlet at all supersonic Mach numbers tested. These expansion waves would cause spillage at the end of the wedges. This spillage would prevent the free-stream tube area from reaching a maximum value for a two-dimensional wedge at any Mach number.

[redacted]

Presented in figure 13 is the variation of the external-drag coefficient with Mach number of model A, model B, and a twin-nacelle ram-jet configuration (ref. 4). A correct comparative evaluation of the drag of the three configurations cannot be made from the results presented in figure 13 alone because of the difference in geometry exclusive of the ram-jet installations. Consequently, in order to evaluate the external drag with respect to the type of ram-jet geometry, it was necessary to make the following adjustments analytically so as to obtain a comparison on the basis of model B: (a) engine cross-sectional areas equal, (b) equal useful volumes, (c) equal wing areas, (d) equal nose cone angles, (e) no canards, and (f) including the additive drag of the open nose inlet.

Shown in figure 14 is the external drag of the configurations where the experimentally obtained drag was corrected so that an evaluation of the drag may be made on a more comparative basis. The details of the method of correcting in order that this comparison could be made are as follows. The external-drag coefficient of reference 4 was corrected to give the external-drag coefficient shown in figure 14. This external-drag coefficient was obtained by reducing the size of the nacelle units and assuming that the drag of these nacelle units is reduced proportionally as the cross-sectional area of the ram-jet engines is reduced. This reduction in size of the nacelle units (26.5 percent) was necessary so that the sum of the cross-sectional areas of the two engines would be equal to the engine cross-sectional area of model A or B. The external-drag coefficient of model A (fig. 14) was obtained by calculating the decrease in drag due to the removal of the canards (ref. 5), the decrease in the drag due to the difference in cone angle, the increase in drag due to the additional wing area needed to make the wing areas equal (refs. 5 and 6), the increase in drag due to the skin-friction drag of the additional 33.3 inches of body length (ref. 6), and the increase in drag due to the additive drag of the inlet. Since model A had an open-nose inlet it was necessary to replace this inlet with the 40° annular-nose inlet of reference 4. The additive drag for the 40° annular-nose inlet was calculated by the method presented in reference 7. Model B, as shown in figure 14, has had no corrections applied to it.

From a qualitative comparison of the external-drag coefficient of the underslung single-inlet ram jet, the two-dimensional twin-inlet ram jet, and the twin-nacelle ram jet, no appreciable difference in the external-drag coefficient could be noted between the different installations of the ram jets on the models of similar geometric size and volume. The external-drag coefficient of the configurations could change greatly with changes in details of the configurations such as inlet surface angle, position of inlets, mass-flow ratio of the duct, and others.

It can be shown that a gross thrust coefficient of 0.85, based on a 5-inch-diameter body, which is greater than any value of external-drag

coefficient for the configurations presented in figure 14, can be calculated for the ram-jet engines. This thrust coefficient was calculated for an altitude of 35,000 feet and a Mach number of 1.80, assuming a diffuser recovery of 87.5 percent and a combustion chamber loss of 4q. This calculated gross thrust coefficient of 0.85 will be more than adequate to accelerate each of the models presented in figure 14.

CONCLUSIONS

Flight tests were conducted to determine the zero-lift external drag of an underslung single-inlet ram-jet missile configuration and a two-dimensional twin-inlet ram-jet missile configuration, each with one exit of equal geometric areas. The external-drag coefficient, based on the cylindrical fuselage cross-sectional area, for the underslung single-inlet ram jet varied smoothly from a peak value of 0.45 at a Mach number of 1.00 to 0.38 at a Mach number of 1.60. The positive 2° fixed incidence of the horizontal canard surfaces was adequate to trim the model near zero-lift throughout the Mach number range investigated.

The external-drag coefficient, based on the cylindrical fuselage cross-sectional area, for the two-dimensional twin-inlet ram jet had a gradual increase from a value of 0.48 at a Mach number of 1.10 to a peak of 0.56 at a Mach number of 1.37 and then varied smoothly to a value of 0.47 at a Mach number of 1.89.

Qualitative comparison of the external-drag coefficient of the underslung single-inlet ram jet, the two-dimensional twin-inlet ram jet, and a twin-nacelle ram jet indicates no appreciable difference in the external-drag coefficient between the different installations of the ram-jet engines on the models of similar geometric size and volume.

Langley Aeronautical Laboratory,
National Advisory Committee for Aeronautics,
Langley Field, Va.

REFERENCES

1. Jackson, H. Herbert: Flight Measurements of the Effects of Surface Condition on the Supersonic Drag of Fin-Stabilized Parabolic Bodies of Revolution. NACA RM L52B26, 1952.

2. Faget, Maxime A., Watson, Raymond S., and Bartlett, Walter A., Jr.: Free-Jet Tests of a 6.5-Inch-Diameter Ram-Jet Engine at Mach Numbers of 1.81 and 2.00. NACA RM L50L06, 1951.

3. The Staff of the Ames 1- by 3-Foot Supersonic Wind-Tunnel Section: Notes and Tables for Use in the Analysis of Supersonic Flow. NACA TN 1428, 1947.

4. Leiss, Abraham: Flight Measurements at Mach Numbers From 1.1 to 1.9 of the Zero-Lift Drag of a Twin-Engine Supersonic Ram-Jet Configuration. NACA RM L52D24, 1952.

5. Puckett, Allen E.: Supersonic Wave Drag of Thin Airfoils. Jour. Aero. Sci., vol. 13, no. 9, Sept. 1946, pp. 475-484.

6. Van Driest, E. R.: Turbulent Boundary Layer for Compressible Fluids on an Insulated Flat Plate. Rep. No. AL-958, North American Aviation, Inc., Sept. 15, 1949.

7. Sibulkin, Merwin: Theoretical and Experimental Investigation of Additive Drag. NACA RM E51B13, 1951.

Horizontal exposed wing area = 109.7 sq in.
Horizontal exposed canard area = 15.1 sq in.
Vertical exposed wing area = 90.6 sq in
Vertical exposed canard area = 9.7 sq in.

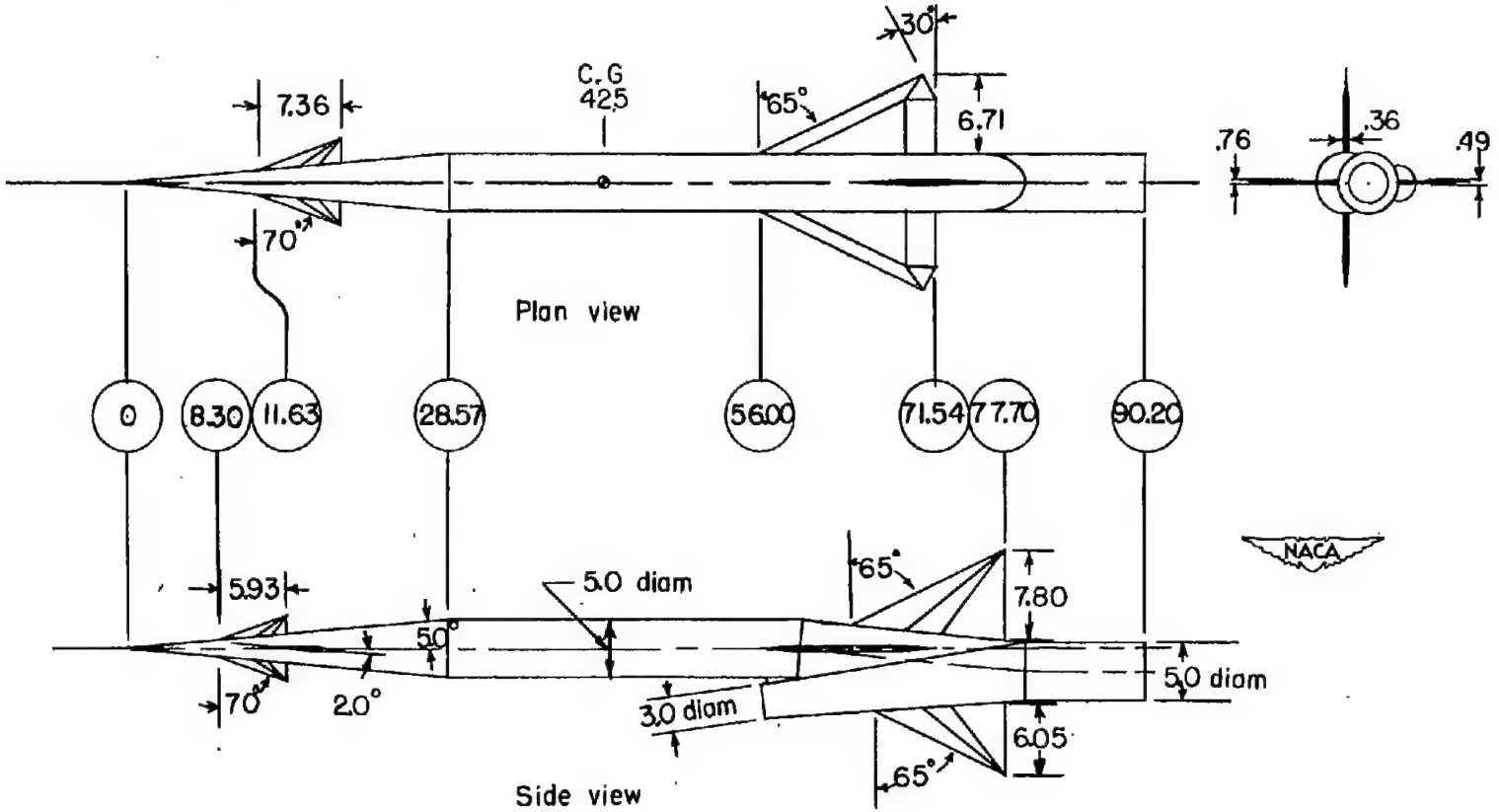

Figure 1.- Sketch of model A. All dimensions in inches.

Horizontal exposed wing area = 174.5 sq in.
Vertical exposed fin area = 162.0 sq in.

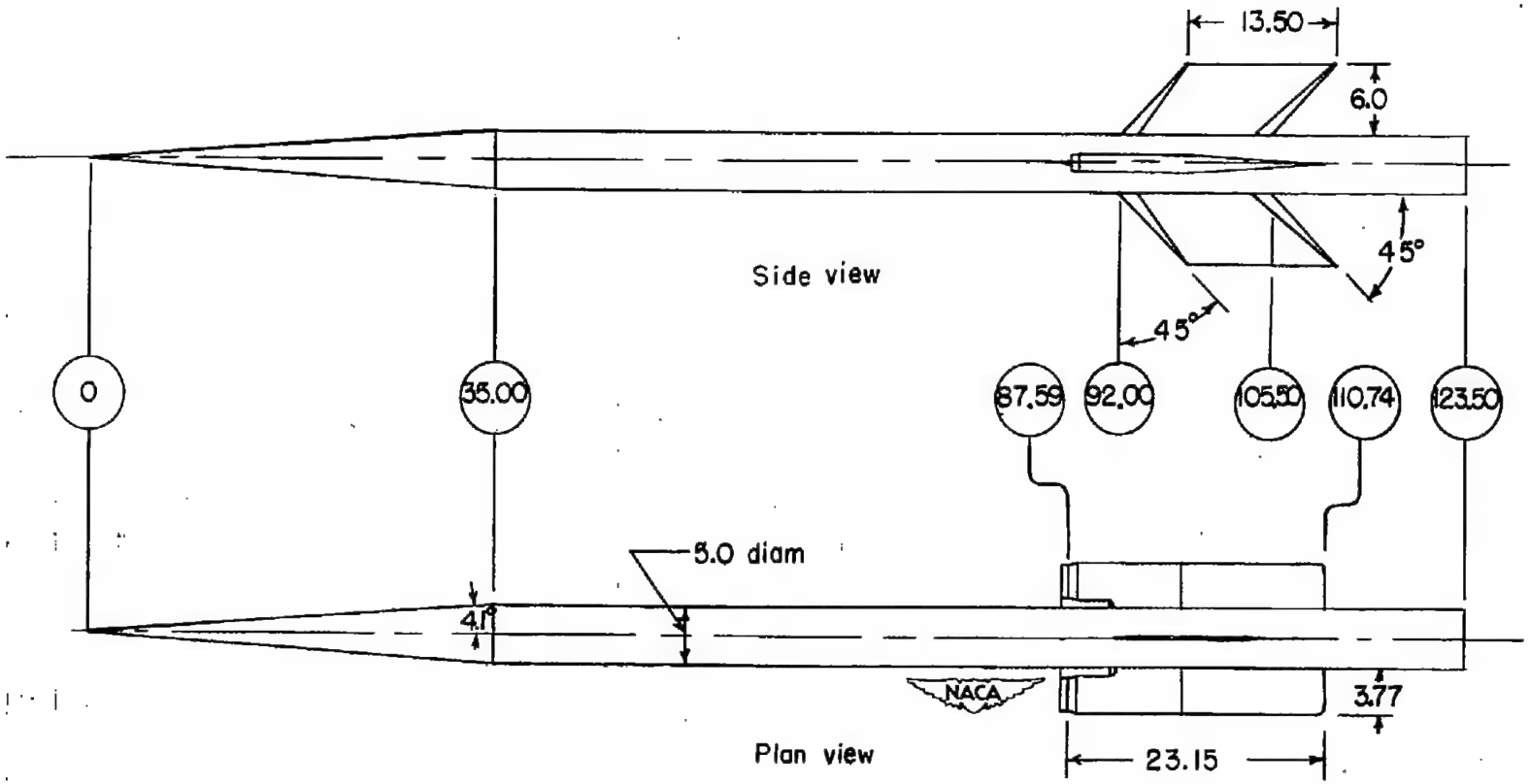

Figure 2.- Sketch of model B. All dimensions in inches.

Side view

Plan view

Figure 3.- Photographs of model A.

NACA L-76990

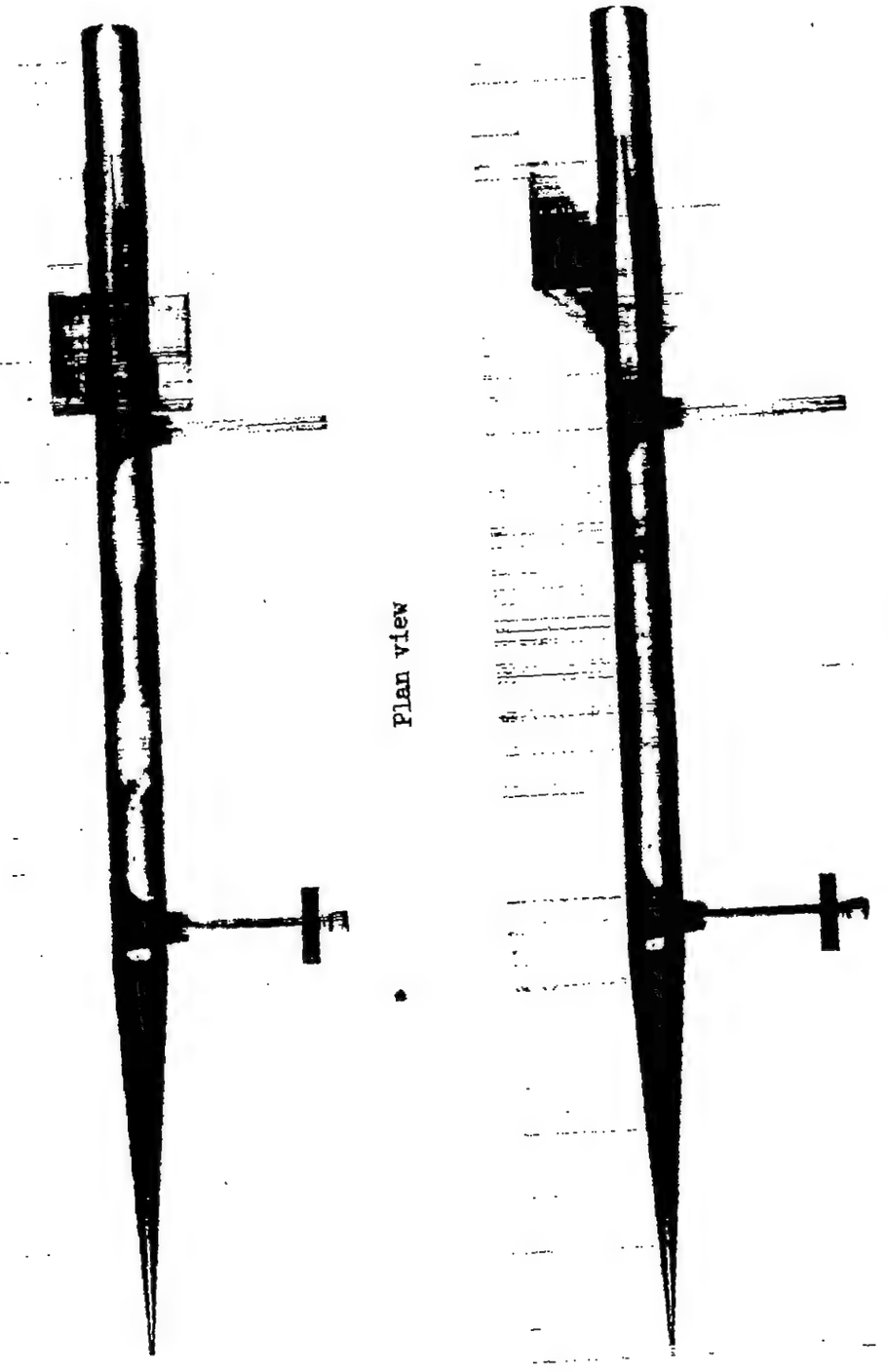

Figure 4.- Photographs of model B.

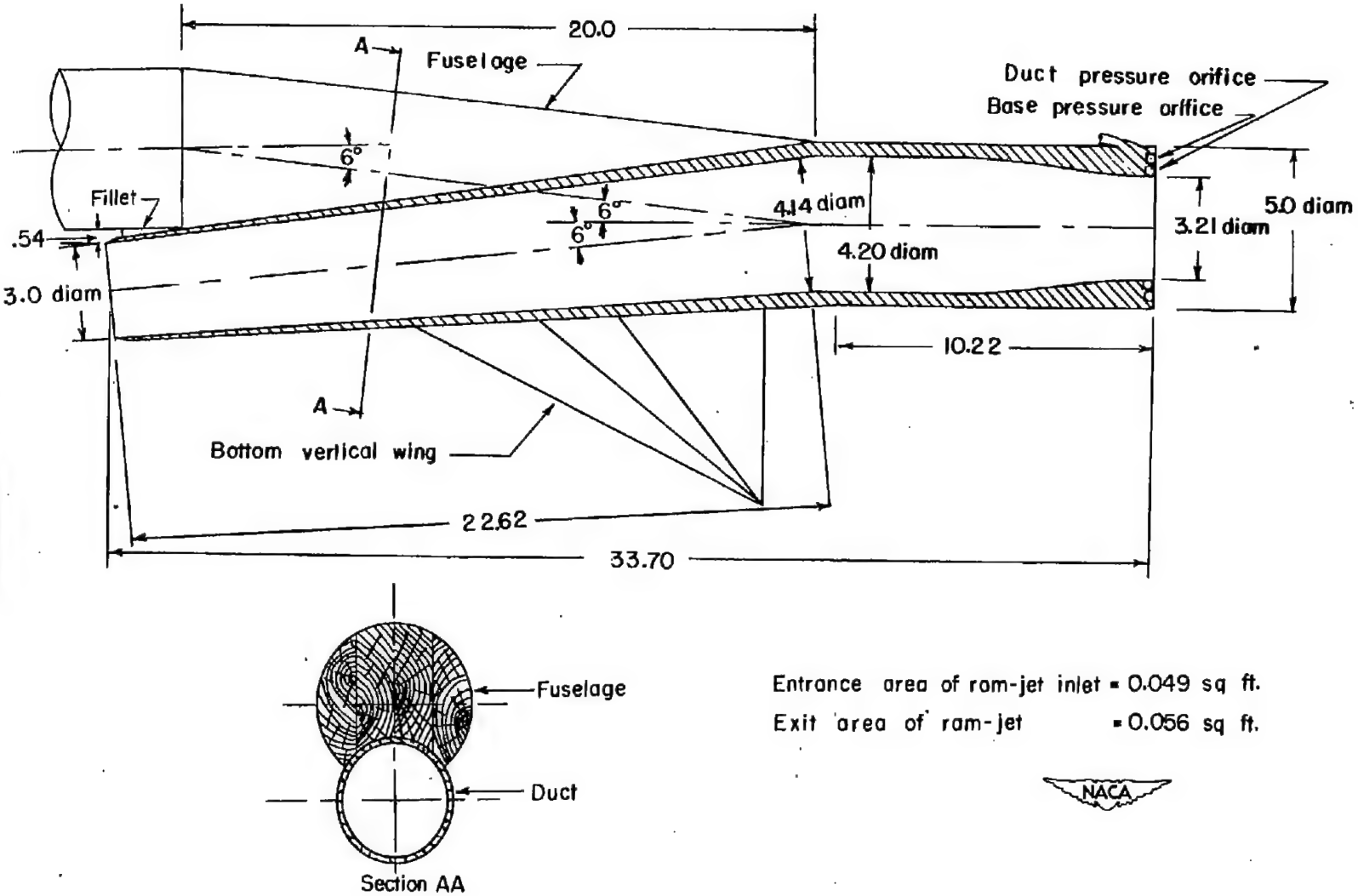

Figure 5.- Internal geometry of inlet and sectional view of fuselage-duct intersection for model A. All dimensions in inches.

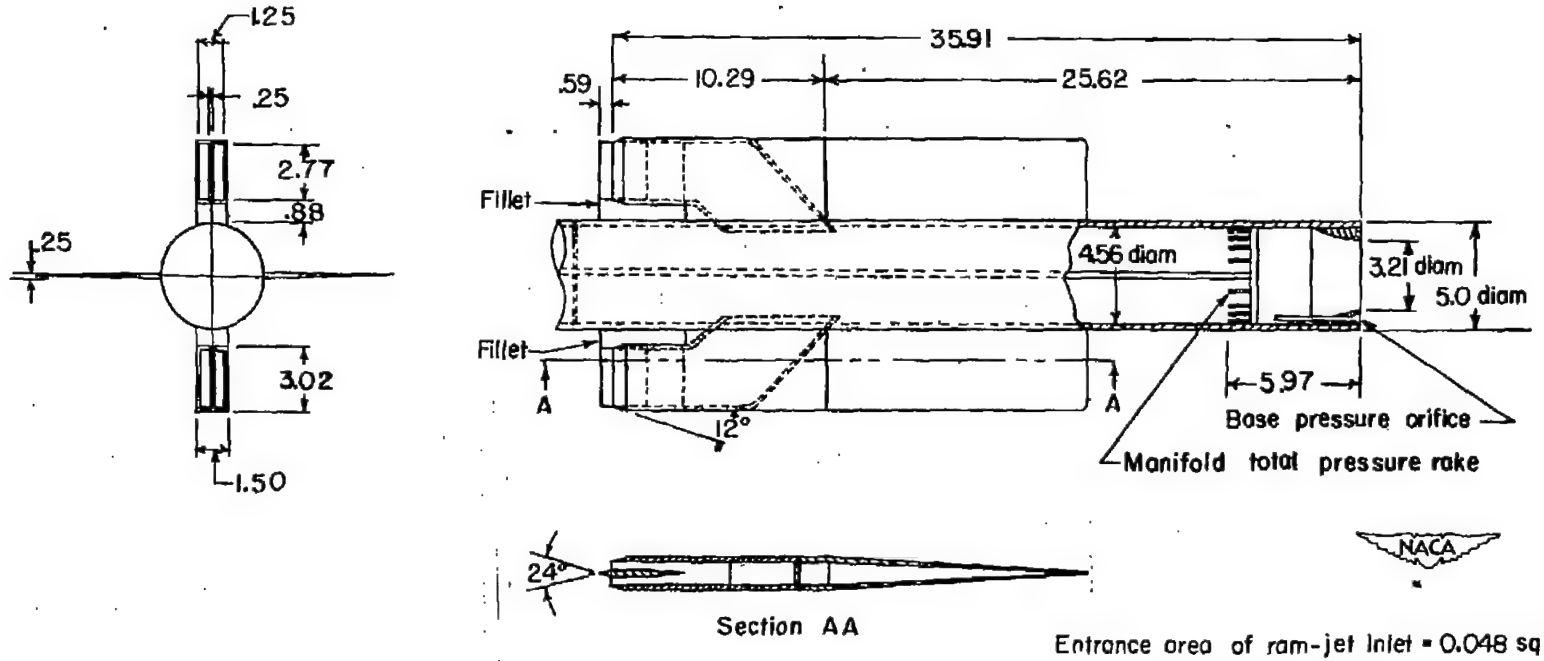

Figure 6.- Internal geometry of two-dimensional inlet for model B.
All dimensions in inches.

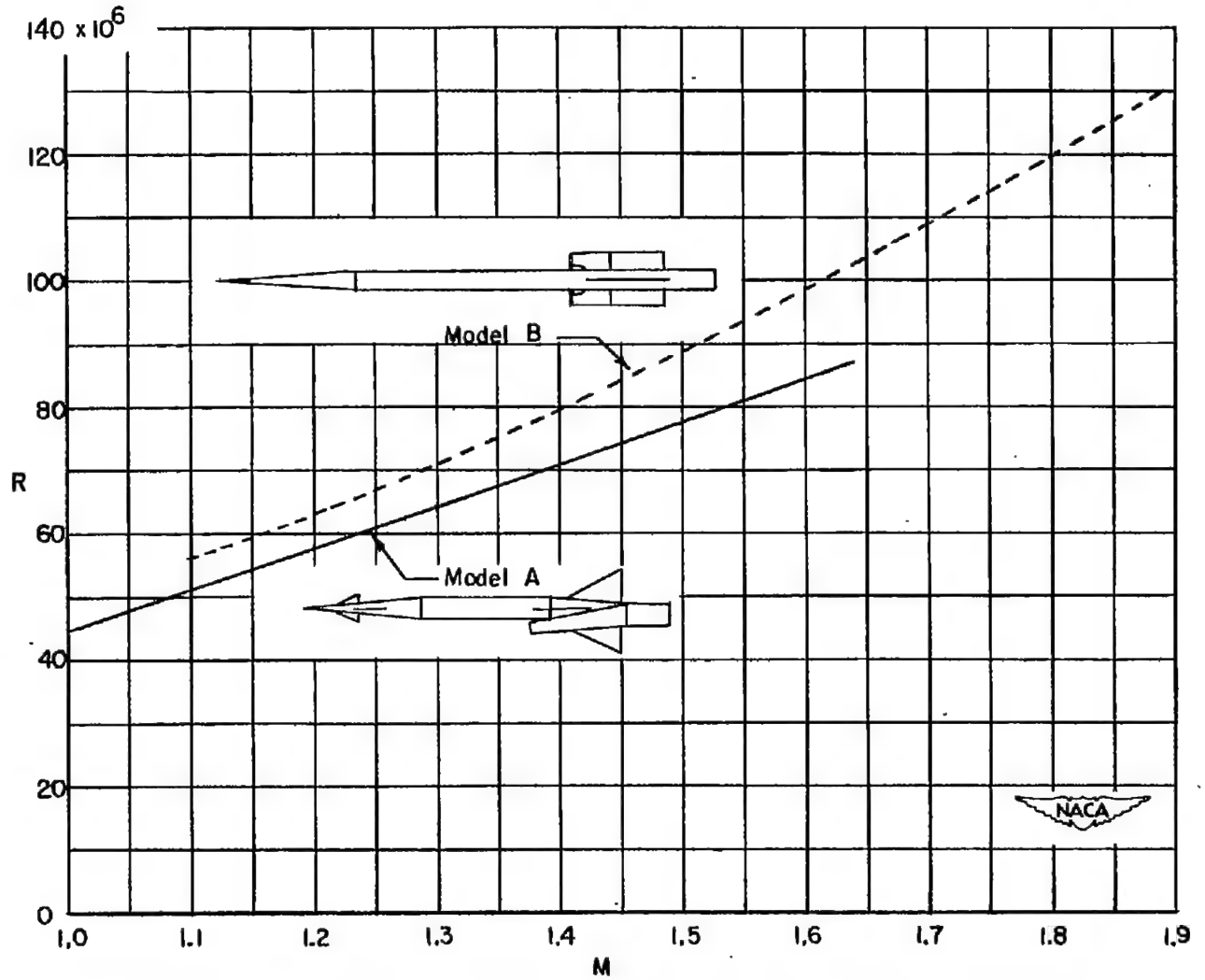

Figure 7.- Variation of Reynolds number with Mach number for models tested, based on body length.

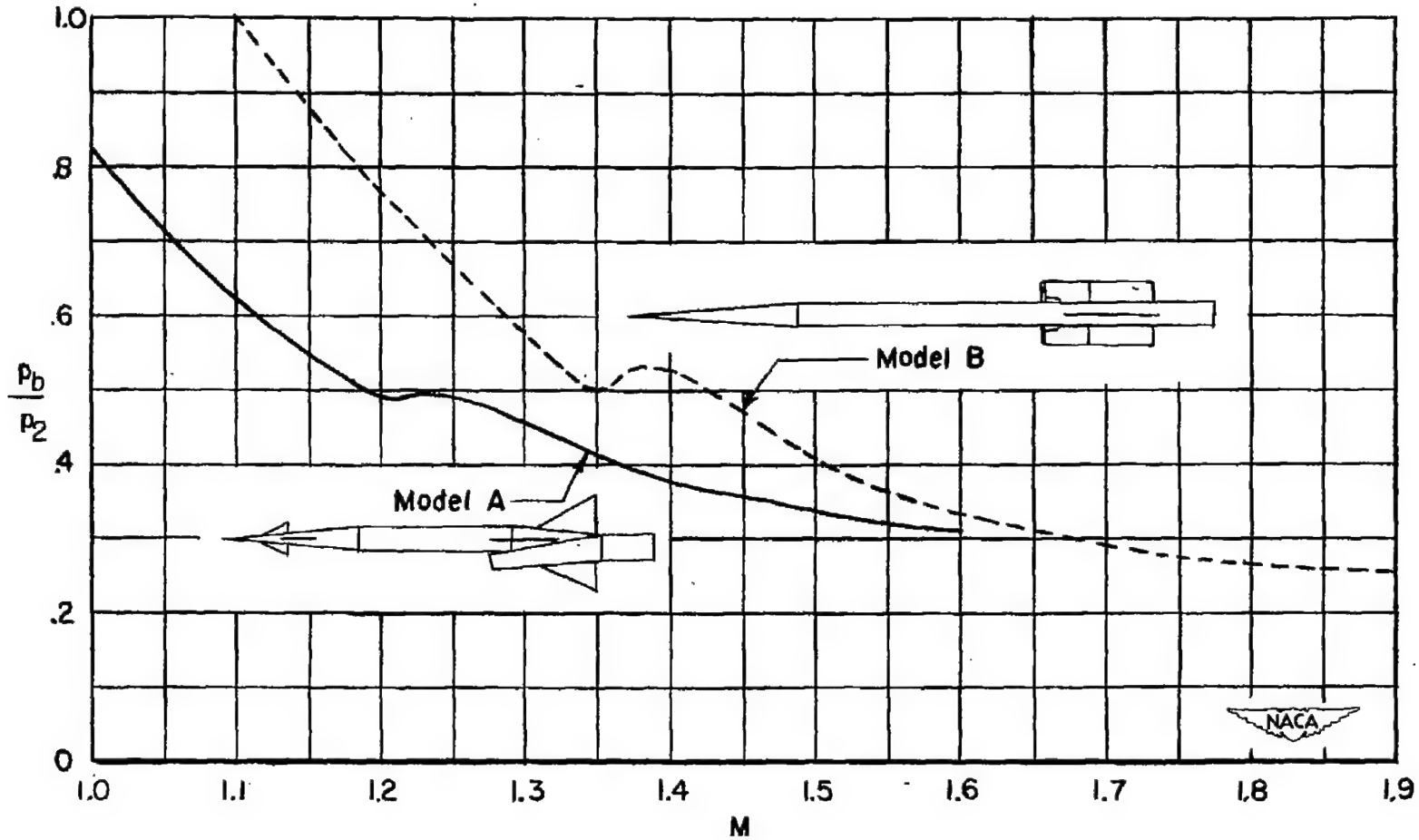

Figure 8.- Variation of the ratio of base pressure to duct exit pressure with Mach number for models tested.

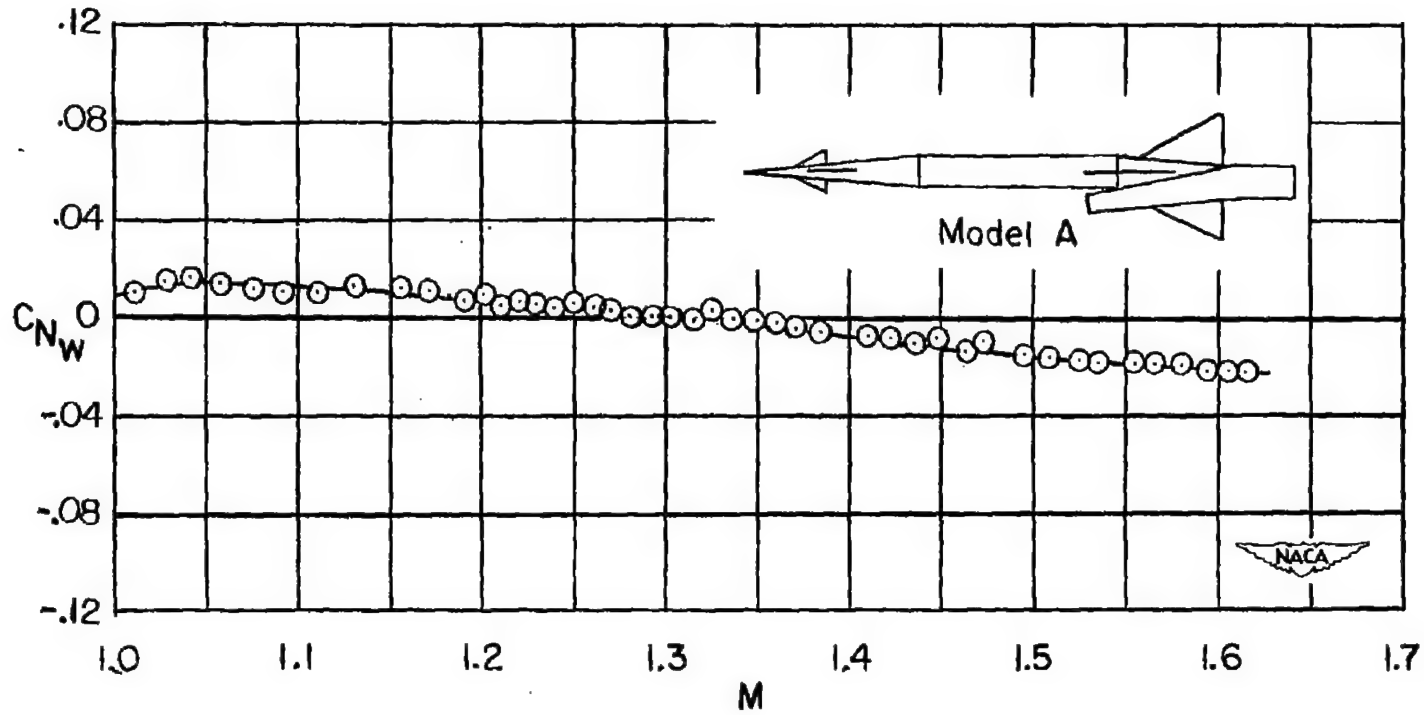

Figure 9.- Normal-force coefficient variation with Mach number for model A, based on exposed wing area.

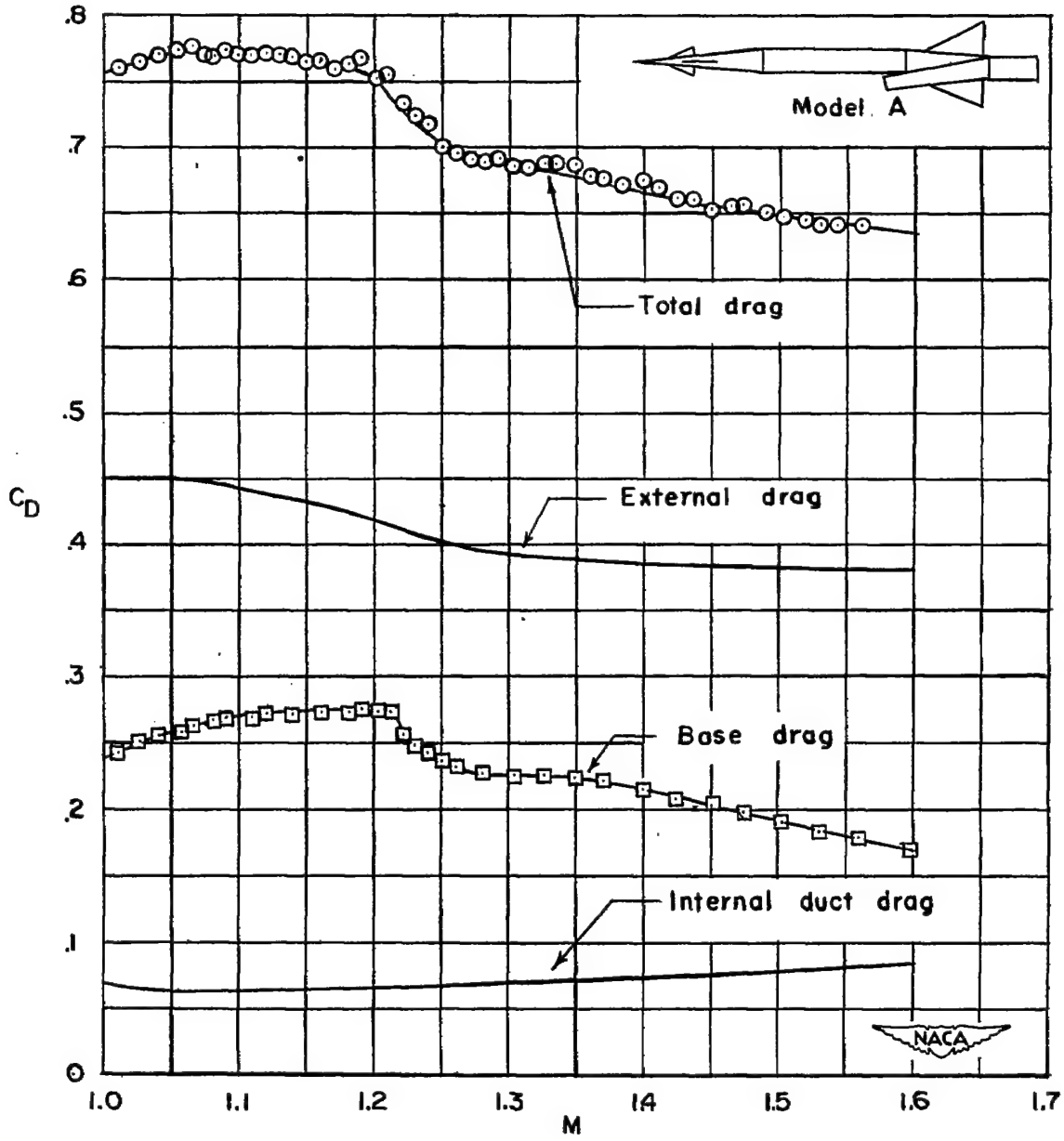

Figure 10.- Drag coefficient variation of total model drag, internal duct drag, base drag, and external model drag with Mach number for Model A, based on fuselage cross-sectional area.

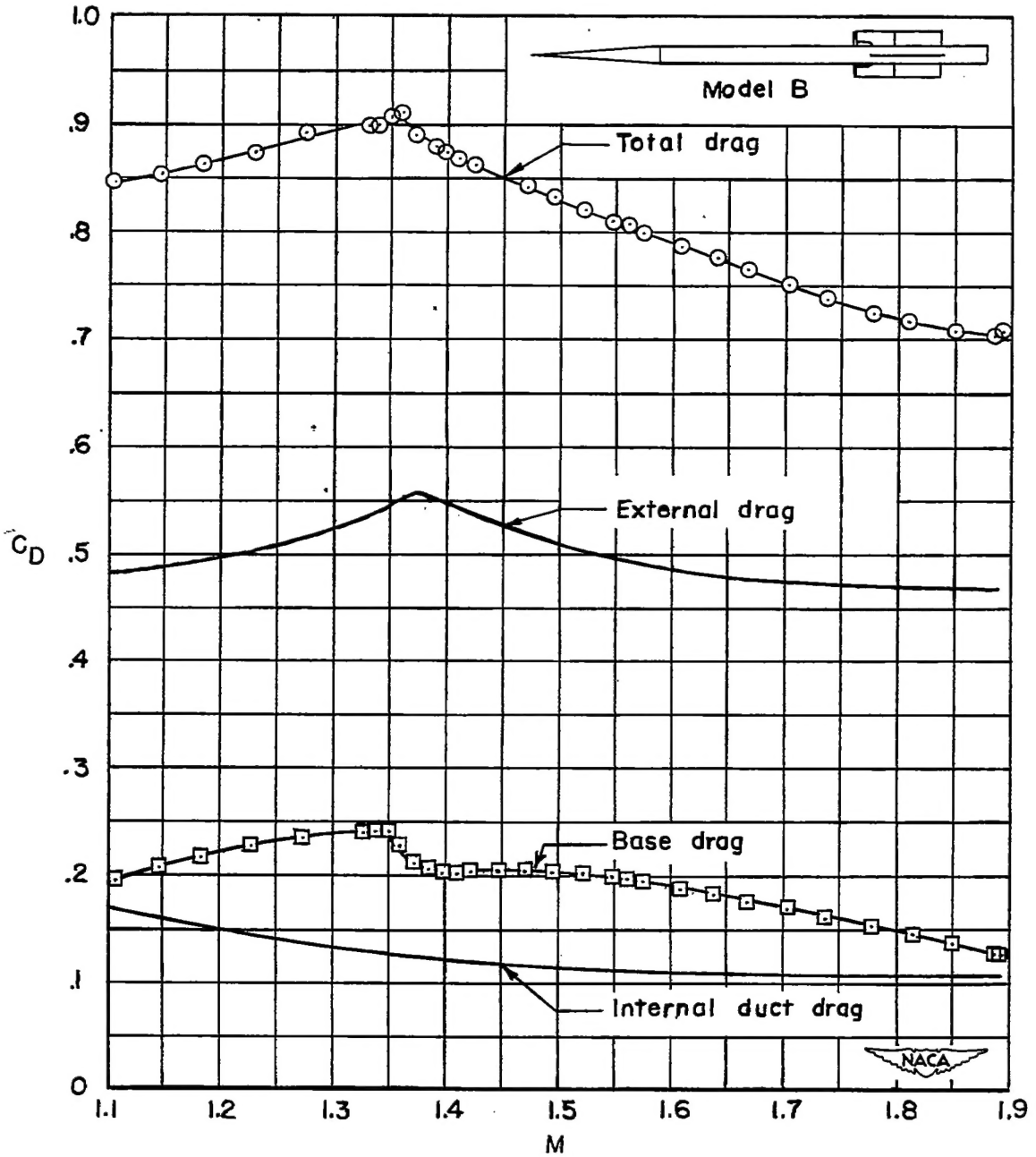

Figure 11.- Drag coefficient variation of total model drag, internal duct drag, base drag, and external model drag with Mach number for model B, based on fuselage cross-sectional area.

[redacted]

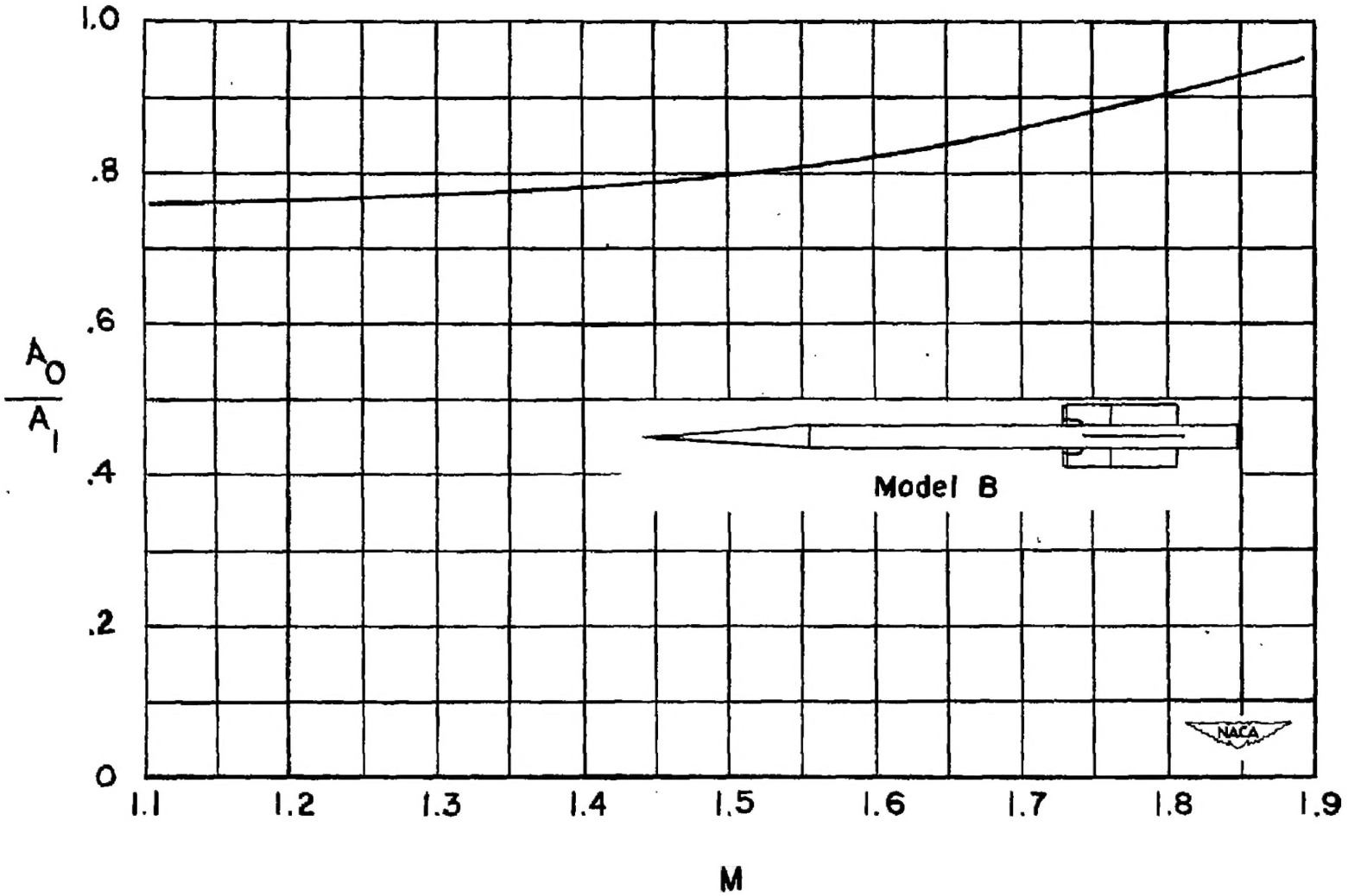

Figure 12.- Ratio of free-stream tube area to geometric entrance area variation with Mach number for model B.

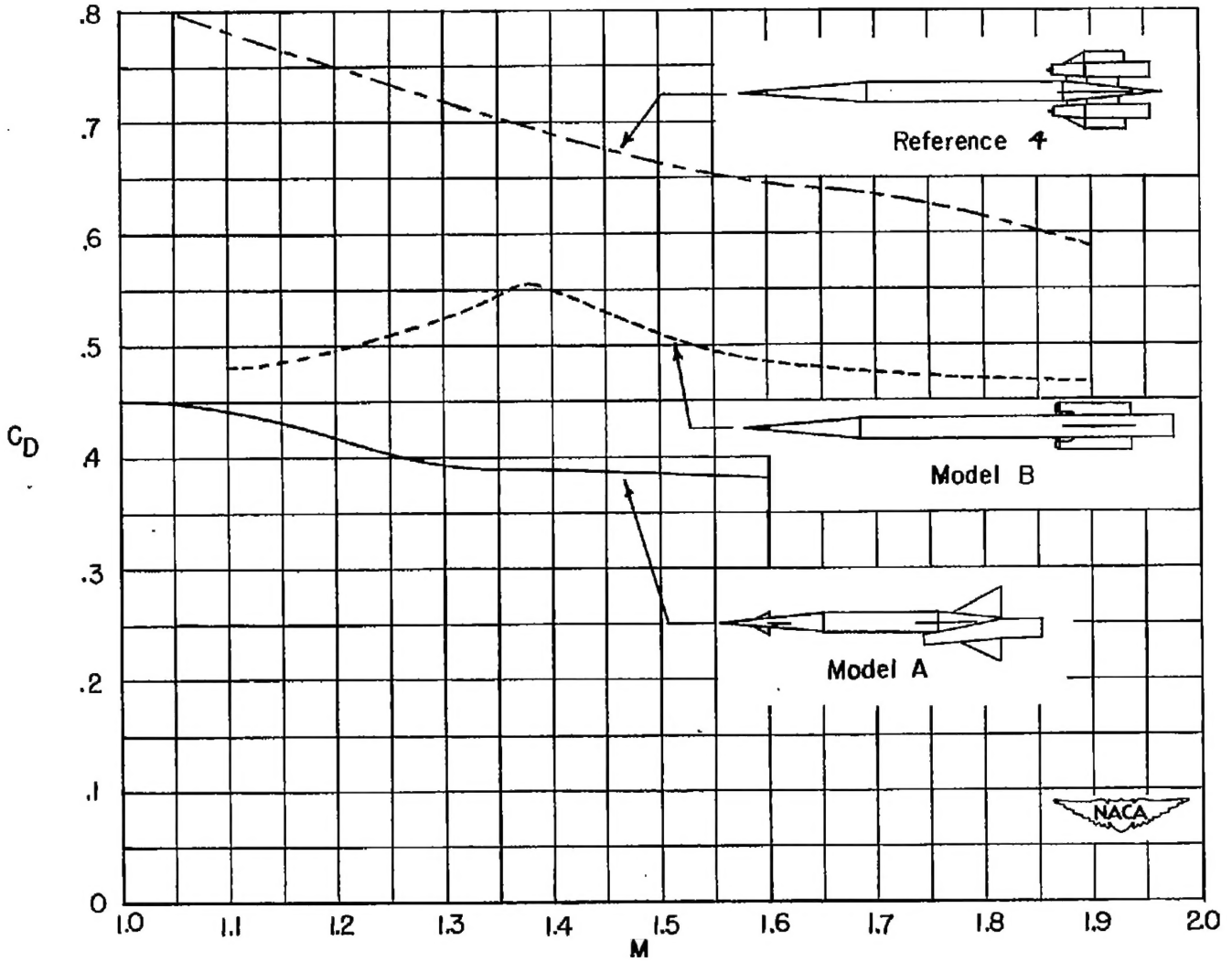

Figure 13.- Variation of the external-drag coefficient with Mach number of model A, model B, and the model presented in reference 4.

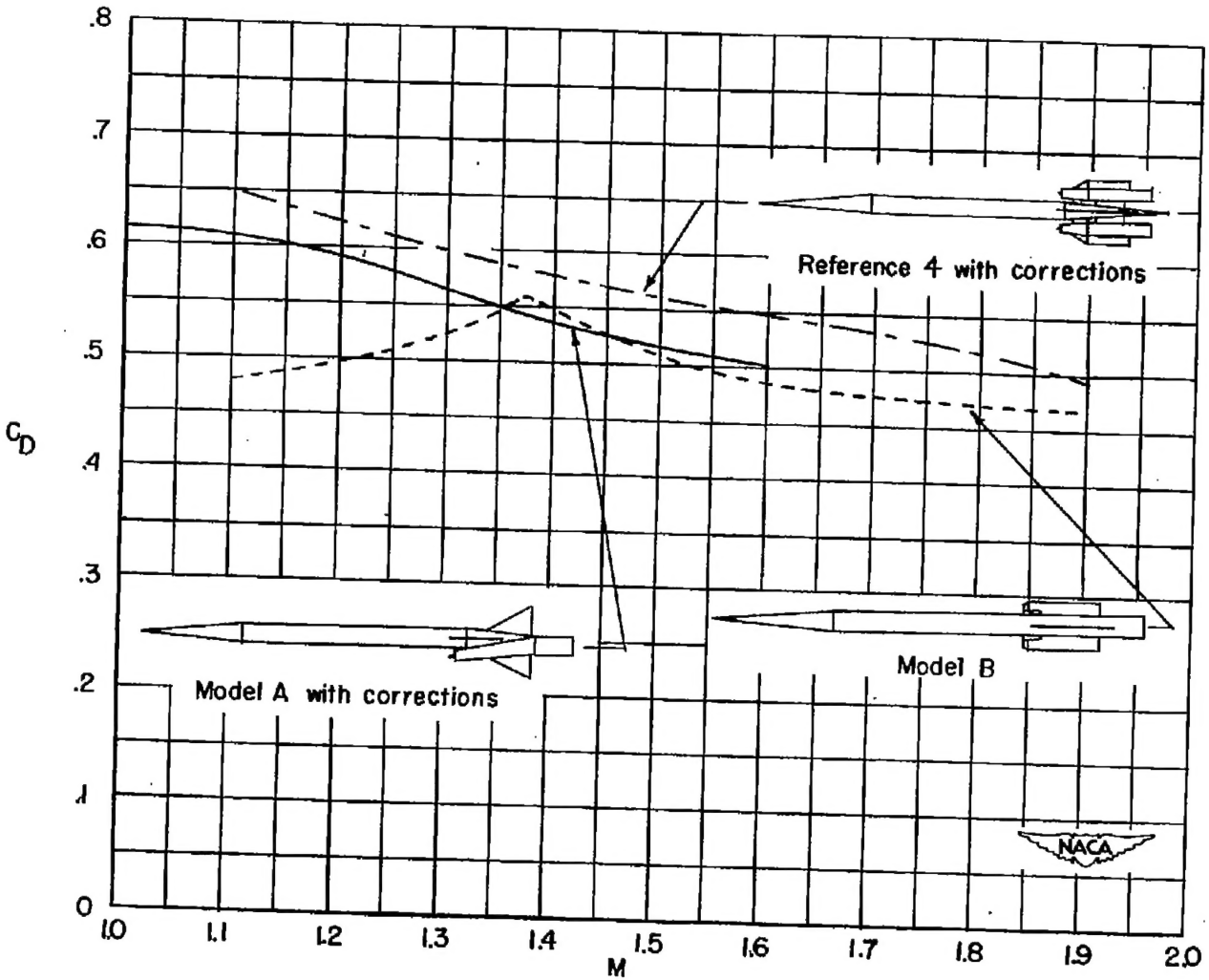

Figure 14.- Variation of the external-drag coefficient with Mach number of model A with corrections, model B, and the model presented in reference 4 with corrections.